Photopharmacology

International Edition: DOI: 10.1002/anie.201813110
German Edition: DOI: 10.1002/ange.201813110

A Photoswitchable Agonist for the Histamine H_3 Receptor, a Prototypic Family A G-Protein-Coupled Receptor

Niels J. Hauwert[+], Tamara A. M. Mocking[+], Daniel Da Costa Pereira, Ken Lion, Yara Huppelschoten, Henry F. Vischer, Iwan J. P. De Esch, Maikel Wijtmans, and Rob Leurs**

Abstract: *Spatiotemporal control over biochemical signaling processes involving G protein-coupled receptors (GPCRs) is highly desired for dissecting their complex intracellular signaling. We developed sixteen photoswitchable ligands for the human histamine H_3 receptor (hH_3R). Upon illumination, key compound* ***65*** *decreases its affinity for the hH_3R by 8.5-fold and its potency in hH_3R-mediated G_i protein activation by over 20-fold, with the trans and cis isomer both acting as full agonist. In real-time two-electrode voltage clamp experiments in Xenopus oocytes,* ***65*** *shows rapid light-induced modulation of hH_3R activity. Ligand* ***65*** *shows good binding selectivity amongst the histamine receptor subfamily and has good photolytic stability. In all,* ***65*** *(VUF15000) is the first photoswitchable GPCR agonist confirmed to be modulated through its affinity and potency upon photoswitching while maintaining its intrinsic activity, rendering it a new chemical biology tool for spatiotemporal control of GPCR activation.*

In recent years, photopharmacology has been gaining momentum as a strategy to optically control biochemical processes.[1] The use of light as an external trigger to change ligand shape and consequently its pharmacological properties allows the probing of biological systems with great spatiotemporal resolution.[2] The azobenzene moiety is often used in photoswitchable ligands[1a] due to its limited size, high photostability, and tunability of the absorption wavelength λ_{max}.[3] Its thermodynamically stable *trans* isomer typically involves a flat elongated structure, whereas its photoinduced *cis* configuration has a bent geometry with a considerably shorter end-to-end distance.[4] Whereas photopharmacology is well established in the field of enzyme and ion channel modulation, it is an upcoming technology for G protein-coupled receptors (GPCRs).[1a] GPCRs constitute one of the largest families of transmembrane proteins, their dysfunction is associated with a plethora of diseases and consequently GPCRs are one of the most successful classes of drug targets.[5] Recently, various GPCRs have been successfully targeted using photopharmacology approaches, including μ-opioid,[6] CXCR3,[7] CB1,[8] H_3R,[9] mGlu5,[10] and GLP1.[11] Yet, almost all these examples include at least one but more frequently two antagonistic/partial agonist isomeric forms. In contrast, freely diffusible affinity and potency photoswitches in which both isomers act as full agonists are scarce,[1a] even though such compounds would be very useful for photopharmacology approaches and complementary to agonist-to-antagonist switches.

The histamine H_3R receptor is an intensively studied GPCR that is known to play an important role in sleep disorders and cognition-related diseases, such as Alzheimer's and Parkinson's disease. The first H_3R antagonist pitolisant (Wakix®) has been approved by the European Medicines Agency for the treatment of narcolepsy.[12] Recently, we published a toolbox of photoswitchable antagonists[9] that competitively inhibit histamine-induced H_3R activity. In the current work, we aimed to develop high-potency H_3R photoswitchable agonists that can simplify spatiotemporal studies of the signaling network of the H_3R. We disclose unique photoswitchable H_3R agonists that can be optically converted to isomers differing in their affinity and potency.

The scaffold design was inspired by the hH_3R full agonist VUF5980 previously published by our lab[13] (Figure 1). To date, virtually every published hH_3R full agonist contains a 4-substituted imidazole moiety combined with a basic or neutral side chain, as is the case for VUF5980. We left the imidazole portion of the molecule unchanged, and considered the diphenylacetylene moiety to be an attractive candidate for an "azologization" strategy.[3] Introducing the azobenzene at this position allows for great flexibility in the diversification of the scaffold. Based on the steep structure-activity relationship observed with VUF5980,[13] it was postulated that small

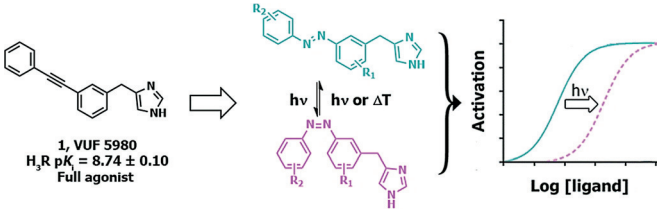

Figure 1. General design and concept of photoswitchable H_3R full agonists.

[*] N. J. Hauwert,[+] T. A. M. Mocking,[+] D. Da Costa Pereira, K. Lion, Y. Huppelschoten, Dr. H. F. Vischer, Prof. Dr. I. J. P. De Esch, Dr. M. Wijtmans, Prof. Dr. R. Leurs
Division of Medicinal Chemistry, Amsterdam Institute for Molecules Medicines and Systems (AIMMS), Vrije Universiteit Amsterdam
De Boelelaan 1108, 1081 HZ, Amsterdam (The Netherlands)
E-mail: M.Wijtmans@vu.nl
R.Leurs@vu.nl

[+] These authors contributed equally to this work.

Supporting information and the ORCID identification number(s) for the author(s) of this article can be found under: https://doi.org/10.1002/anie.201813110.

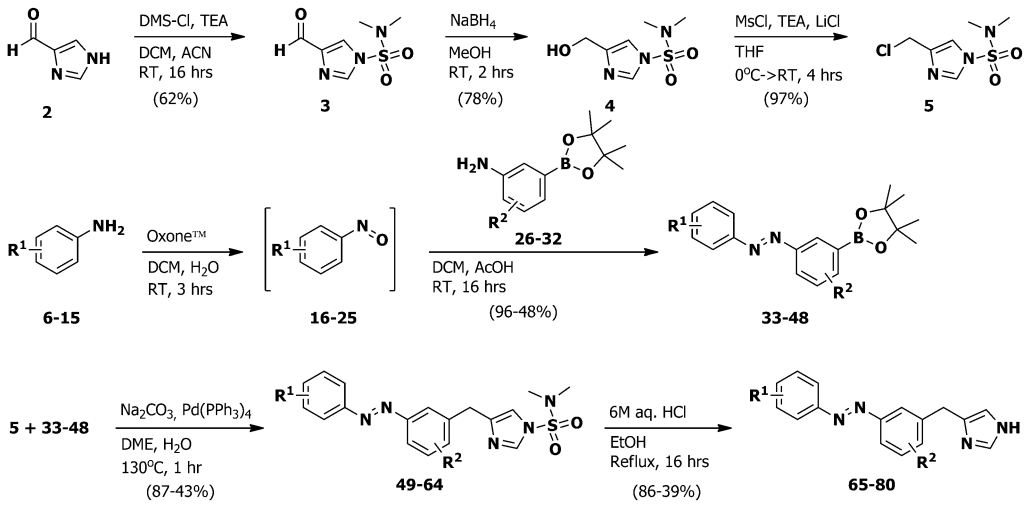

Scheme 1. General synthetic scheme for photoswitchable H_3R agonists. See the Supporting Information for detailed experimental procedures.

changes would have significant impact on the affinity and potency for hH_3R. Therefore, primarily the azobenzene was decorated with small substituents (i.e., methyl and fluorine groups) on both phenyl rings.

To synthesize the ligands, imidazole-4-carbaldehyde **2** was protected using *N*,*N*-dimethylsulfamoylchloride (DMS-Cl, Scheme 1) to afford **3**, which was reduced to **4**. Alcohol **4** was converted to chloride **5** using in situ mesylation. A diverse set of anilines **6–15** was oxidized to the corresponding nitrosobenzenes **16–25** using Oxone™. After work-up, they were directly used in a Mills reaction with 3-amino-phenylboronic acid pinacol esters **26–32** to yield azobenzene–pinacol esters **33–48.** Cross coupling with chloride **5** afforded **49–64** in generally good yields. Acidic deprotection yielded final compounds **65–80**, which were used for biological evaluation.

Table 1: Structure-affinity relationship and photochemical properties of photoswitchable azobenzene-derived H_3R agonists.

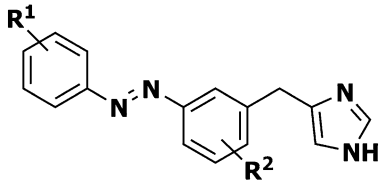

Compound number	R^1	R^2	pK_i *trans* ± SEM	pK_i at PSS *cis* ± SEM	pK_i shift ± SEM	λ_{max} *trans*[b] [nm]	λ_{max} *cis*[b] [nm]	$t_{1/2}$[c] [days]	PSS[d] ± SEM
1	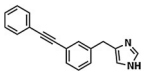		8.74 ± 0.10[a]		–	–	–	–	–
65	H	H	8.42 ± 0.04	7.49 ± 0.05	−0.93 ± 0.06	320	427	106	96.1 ± 1.9
66	2-F	H	8.28 ± 0.08	7.09 ± 0.03	−1.19 ± 0.04	323	425	128	95.7 ± 0.27
67	3-F	H	8.35 ± 0.09	7.42 ± 0.05	−0.93 ± 0.04	320	425	101	94.1 ± 1.3
68	4-F	H	7.69 ± 0.08	6.51 ± 0.08	−1.18 ± 0.09	322	426	95.9	95.9 ± 1.6
69	2,6-F	H	8.00 ± 0.02	7.26 ± 0.09	−0.74 ± 0.10	313	417	26.6	82.6 ± 1.9
70	2-Cl	H	7.86 ± 0.03	6.85 ± 0.04	−1.02 ± 0.03	324	420	96.1	95.3 ± 0.22
71	4-Cl	H	6.76 ± 0.07	5.98 ± 0.07	−0.78 ± 0.10	326	428	29.7	97.5 ± 0.48
72	H	2-Me	5.57 ± 0.09	5.45 ± 0.03	−0.12 ± 0.10	323	428	147	92.3 ± 4.9
73	H	4-Me	6.90 ± 0.06	5.77 ± 0.13	−1.13 ± 0.08	327	430	42.9	96.3 ± 1.1
74	H	5-Me	5.75 ± 0.03	5.13 ± 0.17	−0.62 ± 0.19	322	427	122	94.5 ± 1.4
75	H	6-Me	7.15 ± 0.03	5.94 ± 0.06	−1.21 ± 0.04	324	426	125	95.8 ± 0.92
76	2-Me	H	7.72 ± 0.03	6.40 ± 0.04	−1.32 ± 0.05	326	426	35.6	96.5 ± 1.6
77	3-Me	H	7.39 ± 0.08	6.46 ± 0.06	−0.94 ± 0.09	323	428	77.0	95.4 ± 0.39
78	4-Me	H	5.72 ± 0.14	5.71 ± 0.06	−0.01 ± 0.16	330	429	34.1	94.0 ± 4.4
79	H	4-F	7.81 ± 0.07	6.54 ± 0.06	−1.27 ± 0.02	324	425	91.7	96.6 ± 0.51
80	H	6-F	8.39 ± 0.06	7.36 ± 0.03	−1.03 ± 0.03	322	427	84.6	94.6 ± 1.3

[a] Adapted from Wijtmans et al.[13] [b] Determined at 25 μM in 50 mM Tris-HCl pH 7.4 buffer + 1% [D_6]DMSO. [c] Thermal relaxation half-life times, as determined by the method of Ahmed et al.[14] in 50 mM Tris-HCl pH 7.4 buffer + 1% [D_6]DMSO, extrapolating to 20 °C. Arrhenius plots are available in Figure S1 in the Supporting Information. [d] Photostationary state area percentages after illumination at 360 ± 20 nm at 1 mM in [D_6]DMSO and as determined by LC-MS analysis at 254 nm. All pharmacology experiments were performed at least in triplicate.

Compounds **65–80** all have λ_{max} values for the π–π* transition of the *trans* isomer between 313 and 330 nm (Table 1). The observed limited variation is due to the absence of strong electron-donating or -withdrawing substituents. Similarly, λ_{max} values for the n–π* transition of the *cis* isomer differed marginally, ranging between 417 and 430 nm. Upon continuous illumination at 360 ± 20 nm, the values for the photostationary states (PSS) of **65–80** ranged from 92.3 to 97.5 % *cis*, except for **69,** which has 82.6 % *cis*. Compounds **65–80** all showed slow thermal relaxation at room temperature (20 °C, Table 1). The observed thermal relaxation half-lives were impractically long for direct quantification, therefore extrapolations of high temperature thermal relaxation were used to quantify half-lives at 20 °C (Table 1 and Supporting Information, Figure S1).[14] Compound **69** showed the fastest thermal relaxation in 50 mM Tris-HCl pH 7.4 buffer, with a half-life of 26.6 days, while **72** showed the slowest relaxation, with a half-life of 147 days.

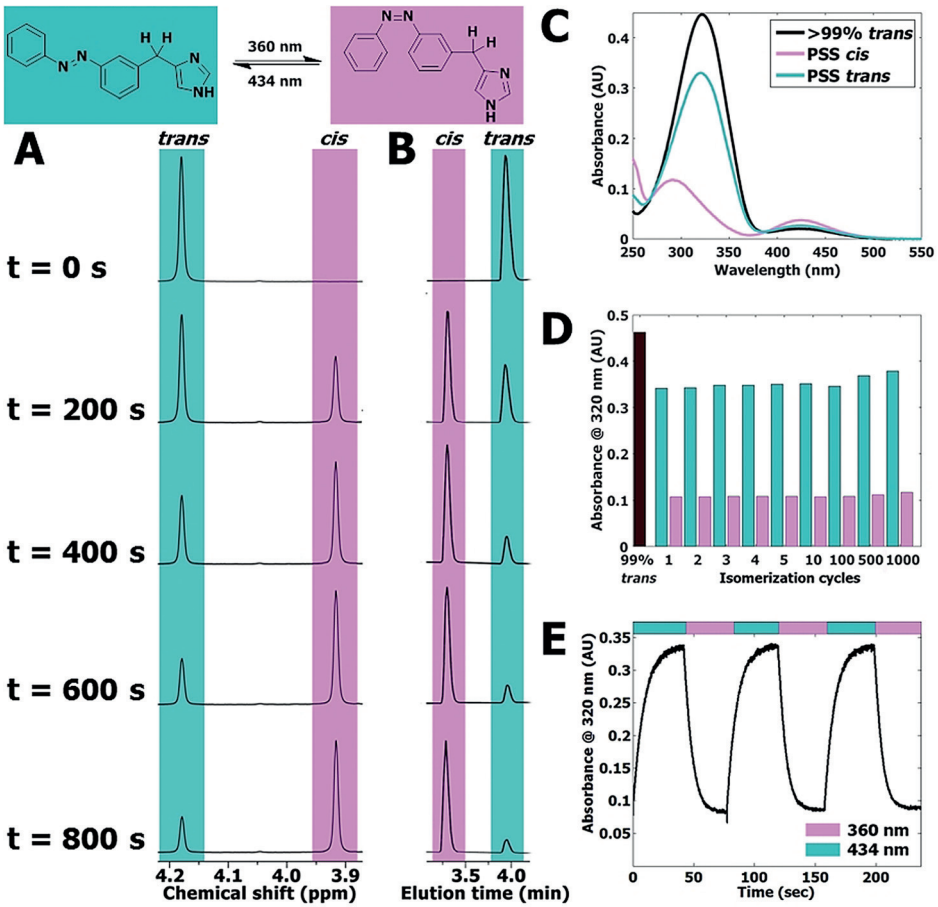

Figure 2. A) Representative part of ^{1}H NMR spectra of 10 mM **65** in [D_6]DMSO illuminated at 360 ± 20 nm displayed at various time points (seconds). The presented peak belongs to the hydrogen atoms explicitly drawn in the structure shown above the spectrum. Full spectra are available in Figure S4 in the Supporting Information. B) Representative part of LC-MS chromatograms belonging to the illuminated NMR sample in Figure 2A. Full chromatograms are available in Figure S5 in the Supporting Information. C) UV/Vis spectra of 25 μM of **65** in 50 mM Tris-HCl pH 7.4 buffer + 1 % [D_6]DMSO. PSS *cis* represents a sample which has been illuminated for 300 s using 360 ± 20 nm light. PSS *trans* represents subsequent illumination for 300 s using 434 ± 9 nm light. D) Repeated isomerization of 25 μM of **65** in 50 mM Tris-HCl pH 7.4 buffer + 1 % [D_6]DMSO analyzed at 320 nm. PSS *cis* was obtained by illuminating **65** for 40 s at 360 ± 20 nm. PSS *trans* was obtained by illuminating **65** for 40 s at 434 ± 9 nm. E) Absorbance at 320 nm of 25 μM of **65** in 50 mM Tris-HCl pH 7.4 buffer + 1 % [D_6]DMSO. UV/Vis spectra were obtained at 1 s intervals under alternating illumination at 360 ± 20 nm and 434 ± 9 nm perpendicular to the light source of the UV/Vis spectrometer.

Based on its favorable pharmacological profile (see below) and synthetic tractability, compound **65** was subjected to in-depth photochemical characterization using ^{1}H NMR and LC-MS analysis during illumination at 360 ± 20 nm. The well-resolved signal of the benzylic CH_2 group provided a clear handle for quantification in ^{1}H NMR analysis (Figure 2A). An overestimation of isomerization percentage is observed in LC-MS analysis at 254 nm compared to ^{1}H NMR analysis (Figure 2B and Supporting Information, Table S1), which can be explained by the differences in extinction coefficients for the *trans* and *cis* isomer at 254 nm (Figure 2C and Supporting Information, Figures S2 and S3). Compound **65** showed excellent resistance to photobleaching during more than 1000 isomerization cycles (Figure 2D). The dynamic isomerization was studied using UV/Vis spectroscopy under alternating illumination (Figure 2E). At 25 μM of **65** in 50 mM Tris-HCl pH 7.4 buffer + 1 % [D_6]DMSO, a half-life of 4.2 ± 0.16 s for 360 ± 20 nm and 5.7 ± 0.19 s for 434 ± 9 nm was observed.

The long thermal relaxation half-lives allowed for detailed pharmacological evaluation using hH_3R competition binding as well as functional experiments. For this, the compound solutions were either illuminated at 360 ± 20 nm to reach a PSS *cis* or kept in the dark to ensure more than 99 % *trans* isomer. The affinity of both isomers for the hH_3R was assessed in competition binding with [^{3}H]-N$^\alpha$-methylhistamine (NAMH). All compounds displayed hH_3R binding affinity, which decreased upon illumination, reaching up to a 21-fold affinity difference in the case of **76**. In terms of absolute affinity, **65** displayed the highest affinities for the hH_3R with a pK_i value of 8.42 ± 0.04 for its *trans* isomer and a pK_i value of 7.49 ± 0.05 for its *cis* isomer, resulting in an 8.5-fold shift upon illumination (Figure 3A and Table 1). Fluorine-substituted analogues **67** and **80** performed similarly to **65** in competition binding, displaying only a marginally lower affinity (Table 1). Notably, *para*-methyl substitution on the R^1

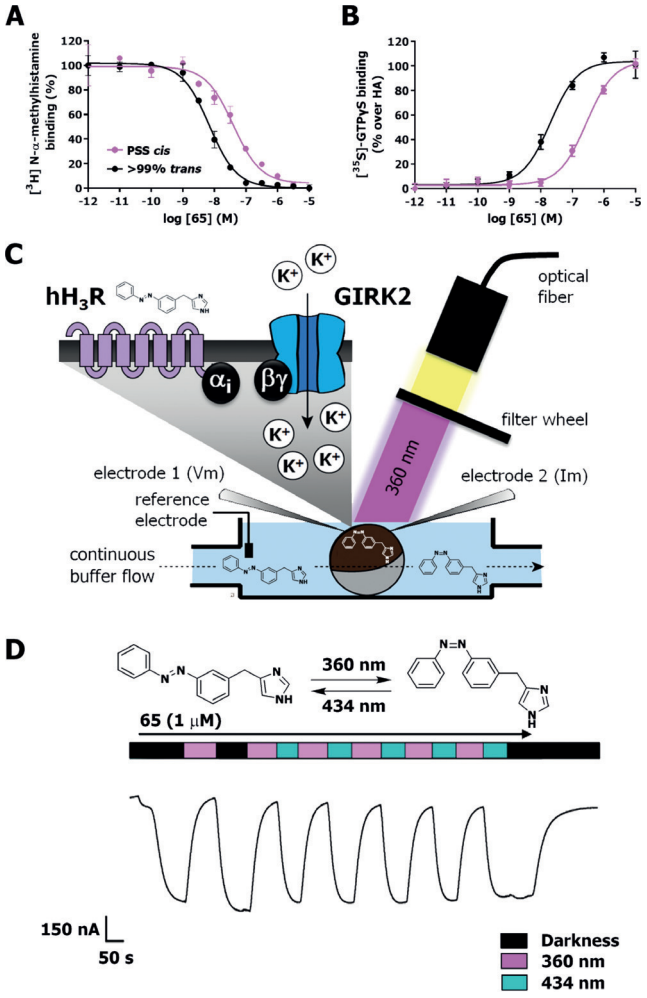

Figure 3. Representative curves of **65** (A) in competition binding with [^{3}H]-NAMH or (B) in G_i protein activation, as measured by [^{35}S]-GTPγS accumulation on HEK293T cell homogenates transiently expressing hH_3R. Black lines refer to a sample containing more than 99% *trans* **65**, while magenta lines refer to a sample of **65** illuminated to PSS *cis* with 360 ± 20 nm prior to the assay. C) Schematic drawing of the TEVC setup used for dynamic hH_3R and GIRK current activation in *Xenopus laevis* oocytes expressing hH_3R and GIRK. D) Representative part of a GIRK-mediated current trace during continuous perfusion with 1 μM **65**, while illuminating the oocyte with alternating 360 ± 20 and 434 ± 9 nm wavelength, as measured by TEVC. Error bars shown are mean ± SD.

position (**78**) decreased the binding affinity and abrogated the photoisomerization-induced affinity shift compared to **65** (Table 1). Reduction of the size of the *para*-substituents to either chlorine (**71**) or fluorine (**68**) moieties gradually rescued hH_3R affinity and reestablished the shift in affinity to 6- and 15-fold, respectively. Methylation at either the *ortho* (**76**) or *meta* (**77**) position of R^1 still resulted in decent binding affinities and high (21-fold) to good (8.5-fold) affinity shifts upon illumination. Addition of substituents at the R^2 position resulted in a clear affinity cliff, with fluorine substitutions (**79** and **80**) still being allowed, but the addition of a methyl substituent (**72**–**75**) highly decreases the binding affinity of the *cis* isomer. Moreover, for the *trans* isomers, 4-Me (**73**) and 6-Me (**75**) substitution was still tolerated yet showed a log-unit decrease in hH_3R affinity compared to **65**, while 2-Me (**72**) and 5-Me (**74**) groups highly reduced hH_3R affinity and consequently reduced or even abolished (**72**) the affinity shift (Table 1).

Based on the observed affinities and photo-induced affinity shifts, the efficacy in stimulating hH_3R-mediated G_i protein activation was evaluated for ligands **65** and **76** in a [^{35}S]-GTPγS binding assay. The highest-affinity ligand **65** (pK_i *trans* = 8.42 ± 0.04) also displayed the highest potency (pEC_{50} *trans* = 7.60 ± 0.13) to induce G_i activation, which upon photoisomerization decreased 20-fold (pEC_{50} at PSS *cis*: 6.30 ± 0.13), with both isomers being full agonists and having intrinsic activities of $\alpha = 1.0 \pm 0.03$, compared to histamine (Figure 3B). Since the observed shift in hH_3R affinity was 8.5-fold, the larger (20-fold) shift in functional potency indicates that for **65** the efficacy (propensity to activate a GPCR[15]) is also affected upon *trans–cis* isomerization. Interestingly, a large photo-induced decrease in potency of 23-fold was also obtained for **76** (pEC_{50} *trans*: 6.78 ± 0.11, PSS *cis*: 5.41 ± 0.11, $\alpha = 1.00 \pm 0.0$). This shift in potency of **76** is completely explained by the observed change of its affinity (see above).

Compound **65** (VUF15000) was selected as tool compound for further analysis, as it has good synthetic tractability and its superior potency is a clear advantage for pharmacological studies. As the imidazole-based pharmacophore/scaffold used in the design of these photoswitchable ligands is prone to interact with other histamine receptor subtypes,[13] **65** was tested for its subtype selectivity. Binding of **65** was more than 300-fold selective for hH_3R over hH_1R and hH_2R (Supporting Information, Table S2), while a 30-fold selectivity was observed over its closest homologue hH_4R (Supporting Information, Table S2). Interestingly, **65** displayed high nM (*trans*) to low μM (PSS *cis*) binding affinities for both mouse and rat H_3R, with a 4-fold and 8-fold shift in binding affinity upon photoisomerization, respectively (Supporting Information, Table S2).

Real-time photomodulation of hH_3R activity by **65** was measured using two-electrode voltage clamp (TEVC) experiments on *Xenopus laevis* oocytes expressing both hH_3R and G protein-coupled inwardly rectifying potassium (GIRK)-channels (Figure 3C). In this expression system, histamine application resulted in hH_3R-mediated GIRK activation, which was insensitive to optical modulation.[9] As expected based on our data with the [^{35}S]-GTPγS binding assay, *trans*-**65** elicited an agonistic response in this system, which could be reduced by switching to the less active *cis* isomer upon illumination at 360 ± 20 nm. Retrieval of the agonistic response could be provoked by either actively switching the *cis* isomer back into its *trans* isomer by illuminating at 434 ± 9 nm or by stopping illumination, due to continuous perfusion of the *trans* isomer (Figure 3D). Dynamic photoswitching of **65** could be performed repeatedly, illustrating that the use of two specific wavelengths allows optical control of the hH_3R activation mediated by **65**. Furthermore, photoswitchable agonist **65** showed rapid hH_3R activation and deactivation kinetics, aiding in its use in in vivo experimentation.

In summary, we have synthesized and characterized 16 photoswitchable hH_3R agonists that change their affinity and

potency upon illumination, indicating a successful azologization strategy. All possess long thermal relaxation half-lives at room temperature making them useful for a variety of pharmacological studies. Compound **65** (VUF15000) was selected as key compound on the basis of synthetic tractability and highest absolute hH_3R affinity. Moreover, upon illumination, **65** displays a high potency and a 20-fold potency shift, while maintaining full intrinsic activity in G_i protein activation, making it especially attractive as a tool compound. With a 20-fold shift in potency, **65** is one of the best photoswitchable GPCR agonists reported so far. Electrophysiology experiments showed the dynamic optical modulation of hH_3R activation induced by **65** in real time, setting the stage for further unraveling of the downstream signaling of hH_3R with great spatiotemporal precision. Recently, photopharmacology approaches with freely diffusible GPCR ligands have, for the first time, been used successfully in vivo to modulate tadpole and zebrafish behavior[10,16] and to elucidate the role of the metabotropic glutamate receptor 4 in the nervous system using a mouse model of chronic pain.[17] In view of the widespread distribution of the H_3R in the central and peripheral nervous system, photopharmacology approaches with tools such as **65** offer new means (complementary to optogenetic approaches[18]) to investigate the spatial and temporal details of H_3R modulation of important processes, for example, arousal, cognition and neuropathic pain.[12a–e]

Acknowledgements

We acknowledge The Netherlands Organisation for Scientific Research (NWO) for financial support (TOPPUNT, "7 ways to 7TMR modulation (7-to-7)", 718.014.002). All authors participate in the European Cooperation in Science and Technology Action CM1207 [GPCR-Ligand Interactions, Structures, and Transmembrane Signaling: A European Research Network (GLISTEN)]. We thank Hans Custers for HRMS analyses, Andrea van de Stolpe for setting up the photochemistry equipment and Fons Lefeber (Leiden University) for NMR assistance. Kristoffer Sahlholm (Karolinska institute) is kindly acknowledged for providing the pcDNA3.1-Kir3.1 and -Kir3.4 plasmids.

Conflict of interest

The authors declare no conflict of interest.

Keywords: agonism · dynamic modulation · H_3R · photopharmacology · VUF15000

How to cite: *Angew. Chem. Int. Ed.* **2019**, *58*, 4531 – 4535
Angew. Chem. **2019**, *131*, 4579 – 4583

[1] a) K. Hüll, J. Morstein, D. Trauner, *Chem. Rev.* **2018**, *118*, 10710 – 10747; b) M. W. H. Hoorens, W. Szymanski, *Trends Biochem. Sci.* **2018**, *43*, 567 – 575.

[2] W. Szymanski, J. M. Beierle, H. A. Kistemaker, W. A. Velema, B. L. Feringa, *Chem. Rev.* **2013**, *113*, 6114 – 6178.

[3] J. Broichhagen, J. A. Frank, D. Trauner, *Acc. Chem. Res.* **2015**, *48*, 1947 – 1960.

[4] A. A. Beharry, G. A. Woolley, *Chem. Soc. Rev.* **2011**, *40*, 4422 – 4437.

[5] a) A. S. Hauser, S. Chavali, I. Masuho, L. J. Jahn, K. A. Martemyanov, D. E. Gloriam, M. M. Babu, *Cell* **2018**, *172*, 41 – 54 e19; b) K. Sriram, P. A. Insel, *Mol. Pharmacol.* **2018**, *93*, 251 – 258.

[6] M. Schönberger, D. Trauner, *Angew. Chem. Int. Ed.* **2014**, *53*, 3264 – 3267; *Angew. Chem.* **2014**, *126*, 3329 – 3332.

[7] X. Gómez-Santacana, S. M. de Munnik, P. Vijayachandran, D. Da Costa Pereira, J. P. M. Bebelman, I. J. P. de Esch, H. F. Vischer, M. Wijtmans, R. Leurs, *Angew. Chem. Int. Ed.* **2018**, *57*, 11608 – 11612; *Angew. Chem.* **2018**, *130*, 11782 – 11786.

[8] M. Westphal, M. A. Schafroth, R. Sarott, M. Imhof, C. Bold, P. Leippe, A. Dhopeshwarkar, J. Grandner, V. Katritch, K. Mackie, D. Trauner, E. M. Carreira, J. A. Frank, *J. Am. Chem. Soc.* **2017**, *139*, 18206 – 18212.

[9] N. J. Hauwert, T. A. M. Mocking, D. Da Costa Pereira, A. J. Kooistra, L. M. Wijnen, G. C. M. Vreeker, E. W. E. Verweij, A. H. De Boer, M. J. Smit, C. De Graaf, H. F. Vischer, I. J. P. de Esch, M. Wijtmans, R. Leurs, *J. Am. Chem. Soc.* **2018**, *140*, 4232 – 4243.

[10] S. Pittolo, X. Gomez-Santacana, K. Eckelt, X. Rovira, J. Dalton, C. Goudet, J. P. Pin, A. Llobet, J. Giraldo, A. Llebaria, P. Gorostiza, *Nat. Chem. Biol.* **2014**, *10*, 813 – 815.

[11] J. Broichhagen, T. Podewin, H. Meyer-Berg, Y. von Ohlen, N. R. Johnston, B. J. Jones, S. R. Bloom, G. A. Rutter, A. Hoffmann-Roder, D. J. Hodson, D. Trauner, *Angew. Chem. Int. Ed.* **2015**, *54*, 15565 – 15569; *Angew. Chem.* **2015**, *127*, 15786 – 15790.

[12] a) R. Leurs, R. A. Bakker, H. Timmerman, I. J. P. de Esch, *Nat. Rev. Drug Discovery* **2005**, *4*, 107 – 120; b) P. Panula, P. L. Chazot, M. Cowart, R. Gutzmer, R. Leurs, W. L. Liu, H. Stark, R. L. Thurmond, H. L. Haas, *Pharmacol. Rev.* **2015**, *67*, 601 – 655; c) M. A. Khanfar, A. Affini, K. Lutsenko, K. Nikolic, S. Butini, H. Stark, *Front. Neurosci.* **2016**, *10*, 201; d) P. Panula, S. Nuutinen, *Nat. Rev. Neurosci.* **2013**, *14*, 472 – 487; e) E. Tiligada, K. Kyriakidis, P. L. Chazot, M. B. Passani, *CNS Neurosci. Ther.* **2011**, *17*, 620 – 628; f) M. Kollb-Sielecka, P. Demolis, J. Emmerich, G. Markey, T. Salmonson, M. Haas, *Sleep Med.* **2017**, *33*, 125 – 129.

[13] M. Wijtmans, S. Celanire, E. Snip, M. R. Gillard, E. Gelens, P. P. Collart, B. J. Venhuis, B. Christophe, S. Hulscher, H. van der Goot, F. Lebon, H. Timmerman, R. A. Bakker, B. I. Lallemand, R. Leurs, P. E. Talaga, I. J. P. de Esch, *J. Med. Chem.* **2008**, *51*, 2944 – 2953.

[14] Z. Ahmed, A. Siiskonen, M. Virkki, A. Priimagi, *Chem. Commun.* **2017**, *53*, 12520 – 12523.

[15] T. P. Kenakin, *Pharmacologic analysis of drug-receptor interaction*, 2nd ed., Raven Press, New York, **1993**.

[16] X. Gómez-Santacana, S. Pittolo, X. Rovira, M. Lopez, C. Zussy, J. A. Dalton, A. Faucherre, C. Jopling, J. P. Pin, F. Ciruela, C. Goudet, J. Giraldo, P. Gorostiza, A. Llebaria, *ACS Cent. Sci.* **2017**, *3*, 81 – 91.

[17] C. Zussy, X. Gomez-Santacana, X. Rovira, D. De Bundel, S. Ferrazzo, D. Bosch, D. Asede, F. Malhaire, F. Acher, J. Giraldo, E. Valjent, I. Ehrlich, F. Ferraguti, J. P. Pin, A. Llebaria, C. Goudet, *Mol. Psychiatry* **2018**, *23*, 509 – 520.

[18] R. H. Williams, M. J. Chee, D. Kroeger, L. L. Ferrari, E. Maratos-Flier, T. E. Scammell, E. Arrigoni, *J. Neurosci.* **2014**, *34*, 6023 – 6029.

Manuscript received: November 15, 2018
Revised manuscript received: January 30, 2019
Accepted manuscript online: February 8, 2019
Version of record online: February 27, 2019

